Phase-based Distance Estimation Integrated With IEEE 802.15.4 TSCH Communication

Grega Morano, *Student Member, IEEE*, Ke Guan, *Senior Member, IEEE*, Andrej Hrovat, *Member, IEEE*, and Tomaž Javornik, *Member, IEEE*

***Abstract*—Localization and sensing inputs are enabling new and improved Internet of Things (IoT) applications and have been studied extensively over the past decade. Unfortunately, many solutions focus primarily on improving localization performance, which in turn reduces communication capabilities. Driven by the Integrated Sensing and Communication (ISAC) aspects, we investigate how localization functionality can be seamlessly integrated into a IEEE 802.15.4 TSCH communication protocol. We present two new methods of phase-based ranging that estimate the distance between two devices with each transmitted data packet. We further analyze the effects of introduced changes on communication, their power consumption, and ranging operability. We improve the state-of-the-art algorithm of phase-based distance estimation by reducing the number of phase samples required, without reducing its accuracy and sensitivity while increasing the energy efficiency.**

***Index Terms*—IEEE 802.15.4, Time Slotted Channel Hopping (TSCH), phase-based ranging, Integrated Sensing and Communication (ISAC), Internet of Things (IoT), AT86RF233**

I. Introduction

CURRENT paradigms for the Internet of Things (IoT) and the sixth-generation mobile communication networks (6G) emphasize multi-functional networks that alongside communication support also sensing and localization functions [1]. Integrated Sensing and communication (ISAC) approaches [2] explore how these functions can be combined into a single integrated system, improving spectral efficiency and providing beneficial mutual assistance. A single combined system also reduces the cost and size of hardware equipment and enables easier network deployment and maintenance, which is especially desirable for large IoT setups. The advantages presented have brought great attention to ISAC and have driven research in multi-functional network design. Classification of such systems recognizes many different approaches [2], [3], including the realization where sensing and communication are co-designed with the aim of meeting the performance requirements of both functions.

This work was supported by the Slovenian Research Agency under grants P2-0016, J2-2507, J2-4461 and BI-BA/19-20-045.

All authors are with the Department of Communication Systems, Jožef Stefan Institute, Ljubljana, Slovenija (e-mail: grega.morano@ijs.si; andrej.hrovat@ijs.si; ke.guan.bjtu@qq.com; tomaz.javornik@ijs.si).

Grega Morano, Andrej Hrovat and Tomaž Javornik are also with the Jožef Stefan International Postgraduate School (IPS), Ljubljana, Slovenia.

Ke Guan is also with the Frontiers Science Center for Smart High-speed Railway System, Beijing Jiaotong University, Beijing 100044, China.

The choice of wireless technologies for an IoT network depends on the application use cases and their requirements. LoRaWAN and NB-IoT are suitable for long-range communication and low-power devices in applications like smart cities or agriculture [4]. In contrast, Bluetooth is well-suited for short-range communication between devices in close proximity, as often used in wearables and home automation [5]. IEEE 802.11 (Wi-Fi) provides high data rates for applications requiring fast data transmissions, such as video streaming or real-time monitoring, while the IEEE 802.15.4 standard defines a set of PHY and MAC protocols designed for low data-rate personal area networks. One of the representatives of the IEEE 802.15.4 standard is the Time Slotted Channel Hopping (TSCH) protocol, introduced in the 2015 revision [6], which significantly improves the packet delivery rate by using the channel hopping technique. It offers high reliability, low or at least predictable delay, and low power consumption, which is perfect for critical low-power applications and the Industrial IoT (IIoT) [7].

Since most of the IoT services are used to monitor the environment, supplementary sensing inputs are beneficial and of great interest, making the ISAC approach the desired feature. The increasing demand for real-time ranging and localization capabilities is enabling new and improved IoT applications, such as asset tracking, indoor navigation, parking management, assisted living, worker safety, smart inventory, warehouse management, etc. Bluetooth 5.1 has already recognized the benefits of adding a sensing function to communications and introduced a packet extension in 2019, that can be used for localization purposes. Similarly, IEEE 802.11az addressed the localization demands by introducing enhancements for indoor positioning in 2022. IEEE 801.15.4a included another PHY mode in 2007, called ultra-wideband (UWB), whose large bandwidth enables high-precision localization. In 2020, IEEE 802.15.4z approved an amendment to the UWB PHY mode that improves the accuracy of localization. The TSCH mode, however, still does not provide sufficient channel sensing functionality, which was the main motivation for this study.

Distance estimation between two devices, which is the first step in many localization approaches, can be achieved with observable parameters that can be extracted from radio communication, including the intensity of the signal, its frequency and phase, and the timing of packet transmission. The IEEE 802.15.4 standard already defines the function of measuring the Received Signal Strength Indicator (RSSI) of a received frame and calculating its Link Quality Index (LQI). Based on the attenuation of the received signal, the distance

to the transmitter can be estimated. Since signal strength metrics are easily obtained after each received packet, their use is generally straightforward to implement and widely accepted [8]. Many RSSI-based localization systems also rely on the fingerprinting technique [9], and with the advent of novel Machine Learning (ML) approaches, the accuracy of such systems is constantly improving [10]. Unfortunately, RSSI measurements are highly susceptible to noise and signal interference and are particularly unreliable in rapidly changing environments, making them unsuitable for high-accuracy solutions. Studies such as [8] and [11], which investigated RSSI-based localization with different wireless technologies, have also shown that RSSI measurements made with other technologies (WiFi and Bluetooth) outperform those made with ZigBee technology, which is made upon IEEE 802.15.4 standard.

The time it takes for a packet to travel from source to destination, known as Time of Flight (ToF), can be used to estimate the range between devices. In the context of narrowband IEEE 802.15.4, Lanzisera *et al.* [12], [13] have demonstrated the use of a two-way ranging technique, that can estimate the distance between devices with an accuracy of 1-3 m. Bedford *et al.* [14] look at ZigBee modules for ToF-based distance measurement in underground tunnels. However, relying on ToF might be problematic because the propagation speed of electromagnetic waves is very high while the distances are relatively short. Even minor measurement errors lead to significant distance errors (one-meter accuracy requires a time resolution of about 3 ns). This is especially observed in narrowband communication, in contrast to UWB technology, whose wide bandwidth allows sub-nanosecond resolution [15].

The challenges of the packet travel time measurements can be mitigated by measuring the phase angle of a radio wave. By measuring the phase difference between the received and transmitted signals, it is possible to estimate the distance between the transmitter and receiver. To avoid initial phase offsets and precise clock synchronization between devices, the Active Reflector (AR) [16] method can be used, where the devices exchange the continuous wave (CW) signal and measure the phase angle both ways with respect to each other. The method is also referred to as two-way phase measurement [17]. To reduce the impact of a multipath environment, devices exchange CW signals over multiple carrier frequencies, expanding the used bandwidth and improving the overall accuracy and resolution of the ranging system.

The IEEE 802.15.4 TSCH protocol natively supports only the RSSI metric, which is extracted during regular data transmission and thus does not affect the main function of the network, i.e., communication between devices. Extraction of other metrics is not supported by the TSCH protocol, and while other solutions primarily aim to improve localization performance, they in turn reduce communication performance. In this article, we propose an improvement to the TSCH protocol that allows the distance estimation between two devices without compromising the ongoing communication. The phase-ranging approach is seamlessly integrated into TSCH, and whenever a data packet is sent, the distance between the receiver and the transmitter is estimated. The solution, therefore, provides two functions using the same hardware and can be realized with commercial off-the-shelf devices, which is cost-efficient and well-suited for IoT setups.

The contributions of this study are summarized as follows.

- Development and integration of novel phase-based distance estimation method into the TSCH communication protocol;
- Adaptation and optimization of the state-of-the-art distance estimation algorithm;
- Implementation and evaluation of proposed approach in three use-case scenarios.

The remainder of this article is structured as follows. In Section II, we present related work that addresses the inclusion of phase measurement in a communication protocol. In Section III, we discuss the challenges of implementing phase measurements in the communication protocol, and then propose two novel implementations in Section IV. In Section V, we present the experimental setup to test the new methods and evaluate their impact on communication, its ranging errors, and energy consumption. Finally, we draw the conclusions in Section VI.

II. Related work

The literature presents many solutions addressing specific issues related to phase-based distance estimation, however, a comprehensive solution that encompasses the ISAC aspects of integrating localization into IEEE 802.15.4 communication is lacking. This section explores the related work in the field, presenting the various solutions proposed for individual problems.

In 2012, Atmel (now Microchip) equipped its IEEE 802.15.4 compliant radios (e.g., AT86RF233) with a Phase Measurement Unit (PMU) that provides a function to measure the phase of the incoming signal [18]. Pelka *et al.* [19] were the first to use the radio to experimentally demonstrate how a distance between two nodes can be estimated from a slope of the measured phase angle. They created an error model and evaluated how the phase measurement is affected by the clock drift of the device, errors in changing the carrier frequency, and the noise generated when sampling the interfered carrier. Using the simple slope extraction approach and phase angle measurements of only two frequencies, they estimated the distance between the devices with the accuracy of 0.02 m in the best case. However, they were only able to estimate the distance in the maximum Unambiguous Range (UR) of 2 meters, since a large frequency step was used.

Oshiga *et al.* [20] proposed to create a large set of phase differences from a small number of measured phase angles, which are sampled at predefined frequencies determined by the Golomb ruler technique. The Efficient Slope Sampling Ranging (ESSR) algorithm was proposed to compare the phase differences with a pre-computed set of phase slopes, and to estimate the distance between two devices. The multiple computed distances were then used for localization of a device. Von Zengen *et al.* [21] presented a Real-valued Distance Estimation (RDE) algorithm that calculates the distance between

two devices using autocorrelation and Fast Fourier Transform (FFT). They presented the InPhase system which sampled 200 frequencies in steps of 0.5 MHz and achieved an accuracy of 0.3 m with the UR of 300 m. In a later paper [22], Schröder *et al.* proposed a Complex-valued Distance Estimation (CDE) algorithm that first computes a complex signal from the measured phases and then applies it to the FFT. To reduce the computational complexity, they proposed to use a smaller bin count and later interpolate the FFT result, while preserving the accuracy of the distance estimation. They showed that the CDE algorithm outperforms the RDE and ESSR algorithms, achieving an accuracy of 0.15 m with the UR of 300 m.

However, none of the proposed methods conforms with the IEEE 802.15.4 communication standard. The RDE and CDE algorithms for example require a large number of measured phase angle samples. To obtain the phase measurement at each frequency in the 2.4 GHz band, the authors proposed to interrupt the communication between two nodes for a certain period of time and measure the phase angles. During this time, the devices are in the "atom routine" and are not available for communication. The network downtime may result in unreliable communication, which is not desirable for time-critical applications. In addition, the measured data from one device has to be sent to the other device after the measurement is complete, which places an additional burden on the communication service and its data throughput.

Bluetooth technology, on the other hand, has already introduced positioning information in Bluetooth Core Specification 5.1, namely the Constant Tone Extension (CTE). A sequence of modulated ones is appended to the end of a packet, which appears as an unmodulated carrier and is primarily used for the measurement of the Angle Of Arrival (AoA) and the Angle Of Departure (AoD). Zand *et al.* [17] used the CTE of a packet for a multi-carrier phase-based ranging solution compatible with the BLE standard, including connection-oriented and connectionless modes of operation. They analyzed the effects of phase sampling intervals between the initiator and reflector, which affect the ranging error. To reduce phase noise and ranging accuracy, which accumulates with time between two phase samples, they proposed a new packet structure called Constant Tone Prefix (CTP), which is prefixed to the response packet. The same authors also introduced one-to-many and many-to-many phase-based ranging, which provides simultaneous distance estimation for all participating devices in a large-scale Bluetooth network [23]. Although some parallels can be drawn, the proposed methods do not comply with the IEEE 802.15.4 communication standard, which uses different packet structures, modulation, message exchange procedures, etc.

III. Challenges of including phase measurements into TSCH communication

The integration of phase-based distance estimation functionality into the TSCH protocol requires a detailed analysis of phase measurement, that have to be considered during the implementation of the solution into the TSCH protocol. In this section, we outline the challenges of phase-based distance estimation and present a comprehensive method for phase measurement that incorporates insights from various research studies.

A. Measuring phase angle

A device can measure the phase angle of an incoming CW signal by comparing the signal's waveform with its local reference. The phase shift between the reference signal and the received signal is proportional to both frequency f and distance d, i.e.:

$$\phi(f,d) = \frac{2\pi d}{c} \cdot f + (2\pi N) + \phi_{off} \tag{1}$$

where c is the speed of light and an integer N represents the cyclic nature of the phase angle as it rotates with period 2π. Since the clock source of the receiver is not synchronized with the transmitters, an additional phase offset ϕ_{off} is induced during the measurement. To remove the influence of the unsynchronized clocks, Kluge *et al.* [16] propose the Active Reflector (AR) technique, which measures the phase of the communication channel in both directions. First, the device called the initiator transmits the local oscillator signal, i.e., a constant tone, and the second device, called the reflector, performs the phase measurement. In the next step, the reflector transmits the constant tone with its local oscillator frequency back to the initiator, which performs the measurement. When the initiator later obtains the measured phase from the reflector, it can merge the two measurements and remove the additional phase offset term:

$$\phi_{AR}(f,d) = \phi_I(f,d) - \phi_R(f,d) = \frac{4\pi d}{c} \cdot f + (2\pi N) \tag{2}$$

The same technique also removes an additional phase term that is generated by the local oscillator, which introduces a random initial phase shift when the hardware resets to a new frequency [19].

To eliminate the cycle ambiguity, the phase measurement is obtained from two different frequencies with a frequency step of $\Delta f = f_{k+1} - f_k$, so that the phase difference becomes:

$$\Delta\phi = \phi_{AR}(f_{k+1}, d) - \phi_{AR}(f_k, d)) \tag{3}$$

By combining the (2) and (3) and solving them for d, the distance estimate becomes:

$$d = \frac{c}{4\pi} \cdot \frac{\Delta\phi}{\Delta f} + (\frac{c}{2\Delta f} N) \tag{4}$$

and the unambiguous range is now equal to $\frac{c}{2\Delta f}$. For example, a frequency step of 5 MHz would result in a maximum distinguishable range of 30 m. To achieve high UR resolution, the frequency step should be smaller.

Phase measurements are sensitive to external disturbances and interference. As radio frequency signals bounce off surrounding objects in the environment, the receiver obtains several copies of the signal, each resulting in a different phase shift. Since apparent multipath components in the system can be affected by changing the carrier frequency, multiple tones in the range of $\{f_1, \ldots, f_K\}$ can be used, so that the phase difference after phase-unwrapping becomes:

$$\Delta\phi = \frac{4\pi d}{c} \cdot (f_K - f_1) = \frac{4\pi d}{c} \cdot \Delta f \cdot K \tag{5}$$

and the estimated distance can be expressed as:

$$d = \frac{c}{4\pi} \cdot \frac{\phi_{AR}(f_K) - \phi_{AR}(f_1)}{\Delta f \cdot K} \tag{6}$$

Combining multiple tones increases the effective bandwidth by a factor of K without decreasing the maximum UR, resulting in higher resolution and accuracy of sensing.

B. Sampling frequency selection

IEEE 802.15.4-2015 standard defines 16 channels in 2.4 GHz ISM band, separated by 5 MHz. Combining the phase measurements with this configuration would produce a wide bandwidth ($K \cdot \Delta f = 80$ MHz). But based on real-world measurements, 16 phase samples are not sufficient for desired resolution due to possible interference and multipath effects. In addition, by using $\Delta f = 5$ MHz, the maximum UR becomes 30 m, which is not enough for outdoor scenarios.

The InPhase system used $K = 200$ samples with the step of 0.5 MHz which results in a UR of 300 m [22]. However, the time to measure phases on 200 frequencies does not fit into the tightly scheduled TSCH timeslot. As reported, in their setup the measurement on one frequency takes up to 244 us, resulting in an interval of 48.8 ms for all tones, which is almost five times larger than the typical timeslot duration of 10 ms. To minimize intrusiveness to the communication protocol, the number of taken samples should be reduced. In addition, even though the authors reported no drop in Wi-Fi performance, sweeping with the constant tone over the entire ISM band causes additional, unwanted interference for communication. Therefore, we seek for a trade-off between a number of sampled phases and the resolution of the ranging system and its UR.

Equation (4) shows that the distance is proportional to the phase slope, or in other words to the ratio between phase difference and frequency step. By following the Golomb ruler technique, a large set of phase differences can be created from a small number of measured phases. For instance, by taking K phase measurements $\Phi = \{\Delta\phi_1, \ldots, \Delta\phi_K\}$ on selected frequencies, the original set can be uniquely expanded into a new set of phase differences $\Delta\Phi$:

$$\begin{aligned}\Delta\Phi = \{&\Delta\phi_2 - \Delta\phi_1, \ldots, \Delta\phi_K - \Delta\phi_1, \ldots, \\ &\ldots \Delta\phi_K - \Delta\phi_{K-1}\}\end{aligned} \tag{7}$$

and their related expanded frequency steps $\Delta F = \{\Delta f_1, \ldots, \Delta f_M\}$, with the power of $M = K\frac{K-1}{2}$ [20]. Described superresolution technique with proposed optimized sampling was proposed in [24] by Oshiga *et al.* and well studied on phase ranging problem in [20]. In later, the authors proposed to sample K = 15 frequencies which results in M = 105 unique phase difference samples. This approach systematically reduces the number of frequencies sampled, thereby reducing measurement delay and power consumption, which is beneficial for a low-power network such as TSCH.

C. Sampling time and clock synchronization

As studied in [17], the phase measurement (and hence the estimated distance) is strongly dependent on the time offsets between the sampling periods. The distance error is sensitive to the initiator end reflector measurement difference delay (T_o), and to the delay between the measurement of two different frequencies (T_f). Since the crystal oscillator used for the system clock and frequency generation is imperfect (drift given in ppm), the sampled phase includes to two additional errors. The first is the consequence of a slightly different generated frequency, which results in a different phase rotation for the same distance. The second error is due to the sampling time difference of the measurement by the initiator and reflector, which is caused by the system clock drift. Since the crystals are imperfect and cause a clock deviation during T_o, this leads to an additional phase shift in the phase samples [17].

The described errors in the distance estimates could be compensated if the crystal drifts are known. Since each device has its own crystal, determining all drifts is a difficult task, especially with a large number of devices in WSNs. To avoid this, we observed that the phase measurement of the initiator and reflector should be performed in the shortest possible interval. We propose to obtain the data on selected frequency by measuring the reflectors and initiators phase successively. Furthermore, to avoid crystal offsets measurements and corrections we propose to measure phases from all of the required frequencies sequentially. Figure 1 depicts the proposed Phase Measurement (PM) process.

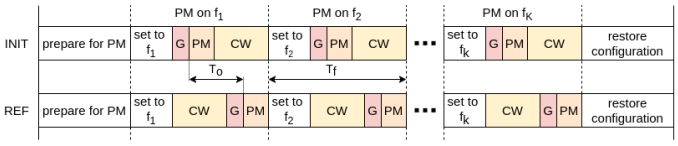

Fig. 1. Proposed phase measurement process between initiator (INIT) and reflector (REF). PM: phase measurement, CW: continuous wave transmission, G: guard interval

Since phase measurement is not part of the normal radio operation during communication, the devices first prepare for the measurement by storing all the register values of the radio and configuring the PMU. The process is exactly the same for both devices, so we assume that the preparation takes the same amount of time. After configuration, the devices start with the phase measurement by setting the local oscillator to a desired frequency (f_1). The reflector then waits for a predefined guard time before measuring the phase, and then transmits a CW. The initiator starts transmitting CW and then waits for a guard time before measuring phase. This method ensures that both nodes measure phase while a CW transmission is in progress. The process is repeated for K different frequencies, and at the end, the nodes reconfigure the radio using the stored register values so that they can proceed with the communication.

D. Constant tone generation

The phase measurement requires that a transmitter sends an unmodulated continuous wave at a constant frequency. For example, Ayyalasomayajula *et al.* [25] extend the data

packet with a stream of 1 or 0 bits that produce a constant tone due to the GSK modulation used. Unlike Bluetooth, the IEEE 802.15.4 standard defines the use of Offset Quadrature Phase Shift Keying (O-QPSK) for the 2.4 GHz band, so a similar approach cannot be used. However, most radios on the market are capable of transmitting an unmodulated carrier, by emptying the frame buffer and configuring the modulation data source to utilize continuous zero or one chip, creating CW. Since this is not a part of the radio's operation during data transmission, the time needed to prepare the radio for CW should be considered when implementing the new approach in the communication timing scheme.

The IEEE 802.15.4 standard also defines the use of TSCH in sub-GHz bands where either OFDM or FSK modulations can be used. While this study focuses on the 2.4 GHz band, a similar approach could be implemented in these scenarios.

E. Synchronization of the measured samples

Another requirement for successful measurement of the AR phase is synchronization between the devices; both devices should start the PM process at the same time. Here we rely on the IEEE 802.15.4 TSCH standard, which by definition builds a globally synchronized network. The communication time is divided into timeslots, typically 10 ms long, which is sufficient to accommodate a data packet transmission and reception, an acknowledgment (ACK) exchange, and all the necessary guard times for packet processing and radio module preparation. Multiple timeslots form a slotframe, a structure that repeats over time as presented in Figure 2. Each timeslot is uniquely identified by its Absolute Sequence Number (ASN), a counter that is incremented at each timeslot. Every node knows the current ASN in the network and therefore knows exactly when to wake up from the low-power operation, and prepare for the communication.

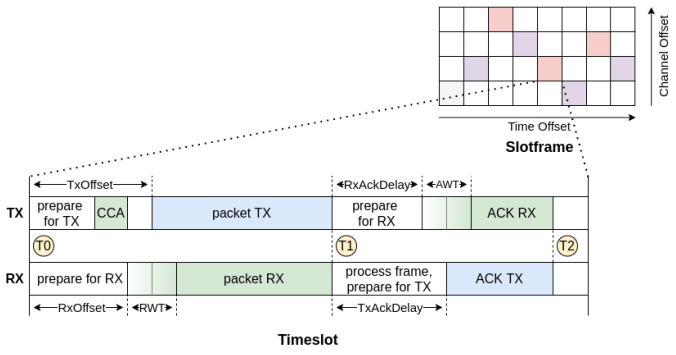

Fig. 2. TSCH default timeslot as part of a slotframe for transmission (TX) and reception (RX) routine (the size of the blocks is not in scale).

Since the nodes exhibit system clock drift due to inaccurate crystal oscillators, it is essential that the nodes periodically correct the drift to their time source. The TSCH utilizes synchronization through pairwise communication: a node synchronizes when it receives a packet or an ACK from its time source neighbor [26]. In the first case, the node timestamps the reception of a packet and calculates the time difference from the expected time. The node then increases or decreases the duration of the current timeslot to compensate for the drift error. In the latter case, the time source calculates the time delta of the reception of a packet sent by the node. The time delta is then included in the ACK so that the node can readjust its current timeslot and compensate for the drift error. Additionally, adaptive time synchronization can be used, where the node learns the relative drift from past synchronizations [27].

To ensure the tight timings within the timeslot itself, the TSCH standard specifies timing template with corresponding delays, as presented on Figure 2. The delays are inputted into timer counters, and their interrupts are utilized for accurate timing operations.

IV. Proposed implementation of phase measurement process

The timeslot shown in Figure 2 is tightly packed with transmission and reception processes, and adding PM process will extend its typical duration of 10 ms recommended in the IEEE802.15.4 standard. Longer timeslots are already included in the Contiki-NG stack to support the slower radios [26]. There is no header-based signaling of timeslot duration within a transmitted frame, so all participating nodes should be configured in advance and consistently for the network to work properly.

For the devices to start the PM process at the same time, there are at least three points in time within the timeslot where synchronization is guaranteed: at the beginning of the timeslot (time T0), after the exchange of the data frame (time T1), and after the exchange of the ACK packet (time T2). We consider the time points T1 and T2 to investigate two non-invasive implementations of the proposed method for effective measurement of the phase angle: phase measurement after acknowledgment and phase measurement after the data packet.

A. Phase measurement after acknowledgment

Inspired by the example of Bluetooth CTE, phase measurement can be seamlessly integrated into the communication protocol by expanding the communication window and adding phase measurement after the ACK packet is exchanged between devices.

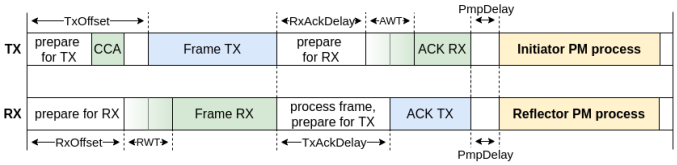

Fig. 3. Extended timeslot including phase measurement after acknowledgment (the size of the blocks is not in scale).

As shown in Figure 3, we define a new short timing delay `PmpDelay` that is added to ensure the devices start the measurement process synchronously. Afterwards, the devices start with the PM process as described in Section III. When the devices obtain the data from all 15 predefined frequencies, they store the measurement along with the ASN, which is later used to combine the samples into the phase differences ϕ_{AR}.

Since the measurement is done only after ACK packets, devices measure the phase of the communication link on every unicast packet. Broadcast packets, which do not require an ACK, are not in our interest because their destination node address is not known. This also helps preserve privacy, because the exact time of PM measurement is not known for a listener outside of the network.

The data obtained by the reflector must be returned to the initiator for the ϕ_{AR} calculation. This can be done within another data packet, but the solution therefore relies on the upper layers (i.e., the application layer), not just on the MAC layer of our interest. Additional feedback data packets increase communication traffic and thus decrease network throughput, since this solution requires the exchange of two data packets for a single distance estimate. With the aforementioned drawbacks in mind, we introduce a new, more efficient approach that addresses the stated problems.

B. Phase measurement after data packet

Each unicast packet in the TSCH network must be acknowledged by the receiver. This feature can be used to send the feedback data to the initiator. The reflector could first obtain the information about the channel and return it back to the transmitter by adding the measured data to the ACK packet. The phase measurement can be encapsulated in the packet using an Information Element (IE), as they provide an adjustable container for additional data to be exchanged between the devices [6]. There are two different types of IEs: (1) a Header IE, which is a part of the MAC header and is not encrypted, (2) and Payload IE, which is a part of the payload and therefore could be encrypted. As defined in the IEEE 802.15.4-2015 standard, the IE is structured with an identification field, a length field, and a content field [6].

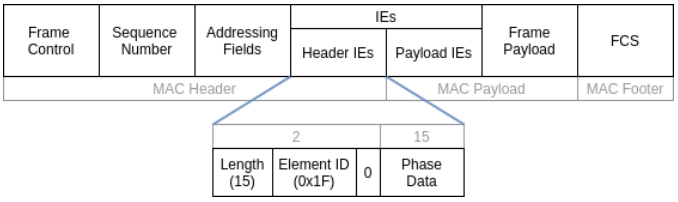

Fig. 4. Enhanced acknowledge frame and added information element structure (the size of the blocks is not in scale).

In the proposed implementation, we are using Header IEs to return the phase information measured with the receiver. We defined new Element ID 0x1F with the name *Phase Measurement*. Its length is set to 15, since we are measuring $K = 15$ samples of phases. The structure of new enhanced acknowledge frame is presented in Figure 4. When TSCH uses encryption, the measured data can be returned to the initiator by using Payload IE which further decreases the possibility of unwanted attacks.

Figure 5 depicts the proposed implementation, where the participating devices first exchange the data packet, then measure the phase and afterward send the ACK packet. The PM procedure cannot be done immediately after frame transmission/reception because the received frame is still in the radios buffer, and the PM setup would discard its content. Therefore, the frame is first obtained and processed. If the ACK is required, the PM process is started. To ensure that the devices start the PM process synchronously, we defined new timeslot timings. The `PmpDelay` value is the same on both devices and should last approximately the same as previously defined `TxAckDelay` (time needed to process the data packet). The new value of `PmpDuration` is equal to PM procedure duration.

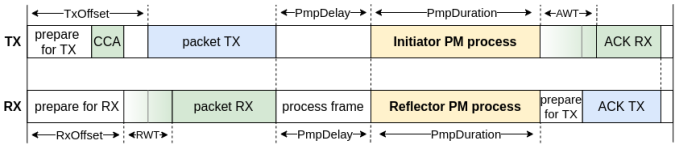

Fig. 5. Extended timeslot including phase measurement after data packet.

The proposed implementation is more intrusive to the TSCH protocol, as less data space is available in the ACK packet, and more changes are introduced at the network stack compared to the PM after acknowledgment implementation. However, in this approach, the data is exchanged between the devices without additional traffic. The phase measurements from both devices are available at the initiator after each packet is sent, which results in high responsiveness and a high refresh rate since a device can induce more phase measurements of a link by sending more packets to a targeted device.

V. Validation of Proposed Implementations

To evaluate the proposed modifications of the TSCH protocol we test them in real-world scenarios by implementing them in the Contiki-NG [28] and its protocol stack. We used VESNA [29] wireless sensor nodes equipped with AT86RF233 transceivers [18]. The radio datasheet contains little information on PMU setup, but a more detail description of the operation can be found in [30].

The used frequency set was generated with the Golomb ruler proposed in [20] and results in: $f_{Golom} = \{2400.5, 2406, 2407.5, 2408, 2412.5, 2423, 2431, 2447.5, 2452, 2460.5, 2463, 2466.5, 2476.5, 2479.5, 2480.5\}$ MHz. The duration of the PM process for a single frequency is equal to $T_f = 420$ us. Measurements at 15 frequencies, together with the time needed for radio preparation and reconfiguration last for 7.9 ms, thus `PmpDuration` time was set to 8000 us. Since the `PmpDelay` should be approximately the same as the previous `RxAckDelay`, we used the same value, which was in our case set to 2000 us. In both proposed implementations, the timeslot duration was extended from the default 10 ms to 20 ms to accommodate the PM process.

A. Effects on communication

The introduced distance estimation techniques shorten the time available for communication which affects the throughput of the network. The number of packets per second (pps) that can be exchanged between two devices correlates with the number of available timeslots per second. The latter is determined by the timeslot duration, size of the slotframe and

its schedule, which are not defined in the IEEE 802.15.4 TSCH standard and are left open to higher levels and implementers, who can adjust their network setup according to the desired requirements and application use cases. To quantify the impact of proposed TSCH modification on the communication, first an ideal TSCH network scenario is modeled, in which a node can utilize all of the timeslots in a slotframe to exchange packets with its neighbor. This schedule would result in a throughput of 100 pps for the typical timeslot duration of 10 ms. In the case where TSCH implements PM after data, less time is available for communication as the timeslot is extended to 20 ms, and the pps ratio drops to 50, reducing the network throughput by a factor of 2. In the case where TSCH implements PM after acknowledgment, the pps ratio drops to 25 because, in addition to extending the timeslot duration, the measurements from the reflector must be sent back to the initiator with an additional data packet that would otherwise be available for application data exchange. The communication load in the network is thus increased, since an additional timeslot is consumed for each measurement feedback, which reduces the overall network throughput by a factor of 4.

The PM after acknowledgment method is also more complex to implement than the PM after data method because it requires a higher layer application, which includes a packet exchange handler to ensure that measurements are efficiently exchanged and later correctly combined using ASN. The PM after data method, on the other hand, returns the measurement from the reflector within the ACK packet to the initiator, so no handler application is required. The MAC layer can compute the ϕ_{AR}, and higher layers can query it after each packet sent. The PM after data method however introduces more changes to the TSCH protocol, because it consumes additional IE of the ACK packet, and defines new timeslot timings for the in-slot synchronization, which are not required for PM after acknowledgment method. Table I summarizes the impacts of the proposed methods on the TSCH communication.

TABLE I
PROPOSED METHODS IMPACTS ON COMMUNICATION

	throughput [pps]	protocol changes	high level application
default TSCH	100	/	/
PM after ACK	25	`PmpDelay`	packet exchange handler
PM after data	50	`PmpDelay`, `PmpDuration`, additional IE	/

The throughput effects could be reduced by shortening the entire PM process, for which a faster signal's phase acquisition is needed. Although the AT86RF233 samples the phase with the interval of 8 us, the radio only supports the Serial Peripheral Interface (SPI) speed of 8 MHz, which is not sufficient for a fast data acquisition. Furthermore, the time needed to configure the radio for CW and to reconfigure it to measure the phase is relatively high, due to low SPI speeds and slow PLL settling times. If the phase measurement would be natievely supported by the hardware (similar to the Bluetooth implementations), the PM process could be shortened, reducing the effects on the network throughput.

It is important to note, that the primary goal of IEEE 802.15.4 and TSCH is not to provide a high throughput, but rather to ensure reliable and energy-efficient communication in low-rate applications. A trade of between throughput and the function of range estimation should be considered regarding the desired application use case, and all devices in the network should be configured the same prior the deployment.

In addition to the affected throughput, it would seem that the transmission of CW employed for channel estimation may affect the usual TSCH communication with additional interference. However, all of the nodes in the network are configured upfront, and even if two devices start the timeslot operations at the same time (at different channel within the slotframe), the communication part of the timeslot will not be affected by the PM part. On the contrary, the communication in other TSCH networks in the vicinity can be affected by introduced ranging, as the networks are not synchronized. With the proposed frequency set, only channels 22 and 26 are directly interfered with the CW transmission. In case the packet exchange happens on those channels while the channel is jammed, TSCH will detect the possible failed attempt and retransmit the packet on a different channel.

B. Ranging performance

In order to demonstrate the viability of the proposed method for ranging, we carried out a measurement campaign during which the devices utilized the PM after data packet implementation. Comparable outcomes can be achieved using the PM after acknowledgment, as the phase measurement results remain consistent regardless of whether they are sampled before or after the acknowledgment. Measurements were made in three different scenarios: outdoors in a park, indoors in an office (5 m x 5 m), and indoors in a hallway (3 m x 40 m). The outdoor scenario was selected as the reference environment with low multipath effects, while the indoor scenarios represent a test environment with possible multipath components and additional IEEE 802.11 interference.

TABLE II
PARAMETERS OF THE EXPERIMENTS

	d_{min} [m]	d_{max} [m]	No. of results	No. of discarded ESSR	No. of discarded iCDE
office	0.5	5.0	3120	660	603
hallway	2.0	20.0	3103	540	1206
park	5.0	100.0	2580	186	547

In each scenario, two VESNA devices were placed on a stand 1.6 m above the floor with clear line-of-sight conditions. The initiator node was connected to a computer to calculate the distance estimates from measured phases. The actual distance between the nodes was measured by laser ranger with an accuracy of $\pm$1.5 mm. The minimal (d_{min}) and maximal (d_{max}) tested distance of separate experimental scenario are shown in Table II. The table also presents the number of

obtained measurements per scenario and number of discarded measurements from different algorithms.

To estimate the distance between the devices, the obtained data was feed to two algorithms: ESSR algorithm presented in [20] and iCDE algorithm presented in [22], which we further adopted to our data collection method. By default, the ESSR algorithm uses only 15 samples of measured phases and compares them with a pre-computed set of slopes. The algorithm outputs a vector of residues and the peak value corresponds to the estimated distance. The number of pre-computed slopes determines the accuracy of the algorithm and the maximum UR. To be comparable to the results in [22], we used 4096 different slope samples with a maximum range of 300 m, resulting in a minimum distinguishable distance of 0.0732 m. The same configuration was used for all three scenarios.

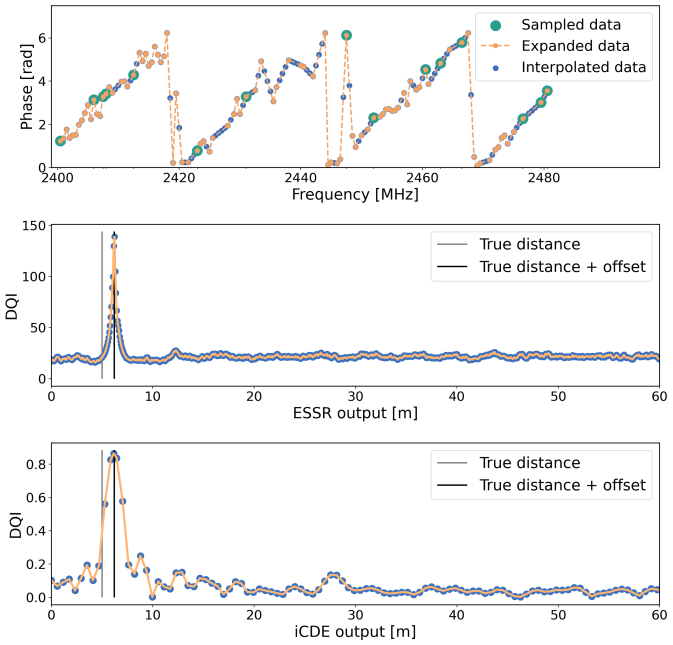

Fig. 6. Example of phase angle measurements at 5 m with corresponding expanded and interpolated data (top), the output from ESSR algorithm (middle), and the output of the iCDE algorithm for the same phase angle measurements (bottom).

iCDE algorithm first computes a complex signal from the measured phases which is then applied to the FFT. By searching for the peak value of the FFT output, the distance can be estimated. The number of used FFT bins is related to a minimal distinguishable distance within the range of the selected maximum range. Schröder *et al.* [22] showed that the number of used FFT bins can be reduced from 4096 to 512 while preserving the accuracy in the UR of 300 m, if the output vector of the FFT is interpolated with polynomial interpolation. The iCDE algorithm, however, requires a larger set of input samples to achieve desired accuracy and sensitivity, thus obtained 15 samples are not enough. As presented with (7), by using phase samples measured at frequencies designed with a Golomb ruler, we can uniquely expand the measured $K = 15$ samples into sets of $M = 105$ samples. Yet, the frequency step of an expanded set of measurements is not equal for each measurement, as seen in Figure 6. To achieve the same sample rate Δf of 0.5 MHz in the whole used spectrum of 80 MHz, we propose to extend the data with linear interpolation. An expanded set of 160 measurements, created from 15 samples can now be fed into the iCDE algorithm.

Both algorithms provide a Distance Quality Indicator (DQI) for each estimated distance, which can be used to rule out erroneous measurements by discarding the ones with a DQI value below a predefined threshold. Using the Youden index, as proposed in the [21], we found that the threshold in our system was 36 for ESSR and 0.41 for iCDE algorithm, resulting in 15.7 % and 26.7 % of the measurements being discarded respectively. Each measurement result contains an additional offset due to the radio signal paths on the circuit board and the antenna. In our case, we measured an offset of 1.1 m, and all measurement results were corrected accordingly. Table III shows the measurement errors from all three scenarios, where the minimum and maximal estimated distance error returned by the algorithms are denoted as min and max consequently. The final median (med), Mean Absolute Error (MAE), and standard deviation (σ) values are calculated as median of the individual values per tested distance, respectively.

TABLE III
MEASUREMENT ERRORS

		min [m]	max [m]	med [m]	MAE [m]	σ [m]
Office	ESSR	-0.989	137.548	0.359	2.127	14.459
	iCDE	-0.707	6.445	**0.254**	**0.527**	**0.950**
Hallway	ESSR	-2.951	110.337	0.259	1.457	9.676
	iCDE	-2.477	1.918	**0.235**	**0.545**	**0.381**
Park	ESSR	-19.962	88.503	0.068	1.470	9.106
	iCDE	-0.339	0.358	**0.065**	**0.088**	**0.083**

Results in Table III show that the office scenario has the highest σ and the highest MAE, while the results of the park scenario can be considered as optimal with respect to the radio channel conditions for the measurements. In addition, indoor scenarios may suffer from interference, as 17 Wi-Fi access points were in operation during the measurement campaign, which was not present outdoors. The results are confirming the conclusion drawn in the [22], where iCDE yields the best results. Our proposed modified version of iCDE, where only 15 phase measurements are needed, is comparable to the original iCDE algorithm and also outperforms the ESSR algorithm. In addition, iCDE requires less computational resources making it the preferred choice for an embedded device.

The better distance estimation performance of the iCDE algorithm can be attributed to better detection of erroneous measurements with DQI value. Upon further examination of the measurement results, we found that both algorithms frequently reported wrong distance estimates at certain locations, due to the influence of multipath propagation and signal reflections from the floor or walls of the building. While iCDE successfully rejects most of the wrong measurements, ESSR fails to detect them, resulting in higher MAE and σ. This is

also confirmed by the reported number of discarded measurements. With the result investigation we also observed, that by using only the DQI value, all outliers in the results cannot be detected. In the case of a mismatch in the measurement process (e.g., erroneous expansion of the measured phases due to noise, the PM measurement is not correctly synchronized, a device misses the time slot, etc.), both algorithms still provide a distance estimate. This value is random and ranges from 0 m to 300 m, which has a large impact on the statistics of the measured data. Since the proposed method makes a distance estimate after each packet is sent, the update rate of the measurement can be high and depends on the interval of sending a data packet to a particular device. This feature offers an option of utilizing additional simple filtering, by using the median of 5 consecutive measurements as the final distance estimation result. The new measurement results using the iCDE algorithm for different scenarios are plotted in Figure 7. As can be seen from the measurement errors listed in Table IV (the additional filtering is marked with the asterisk symbol *), the accuracy and sensitivity of the system are greatly improved.

TABLE IV
MEASUREMENT ERRORS WITH FIVE SUCCESSIVE MEASUREMENTS

		min [m]	max [m]	med [m]	MAE [m]	σ [m]
Office	ESSR*	0.090	0.505	0.341	0.327	0.070
	iCDE*	0.116	0.465	**0.255**	**0.316**	**0.041**
Hallway	ESSR*	-0.044	0.479	**0.174**	**0.245**	0.084
	iCDE*	-0.022	0.267	0.217	0.393	**0.061**
Park	ESSR*	-0.108	0.134	0.061	0.054	0.061
	iCDE*	-0.060	0.078	**0.048**	**0.053**	**0.033**

C. Energy consumption

IEEE 802.15.4 TSCH is intended for use in low-power applications where device energy consumption is of great importance. To analyze the impact of the introduced ranging implementations on energy consumption, we measured the current consumption of the radio using the onboard shunt resistor and shunt amplifier. We used the maximum packet size and presented only the transmission routine since the PM process in the reception routine is similar. In addition, only PM after data packet is presented as the energy consumption of the PM after acknowledgment method is the same. Figure 8 shows the measured current consumption in a transmission timeslot, where four states of the radio can be identified: initialization of the radio, data transmission, phase measurement process, and acknowledge reception. During the PM process, the current consumption changes rapidly as the radio consumes 10.0 mA in the receive mode, 12.8 mA in the transmit mode, and 5.2 mA when powered on [18]. Considering the time required for each state, the radio consumes an average of 179.2 uWs during the PM process, which is roughly the same as the radio's power consumption during the maximum length packet transmission

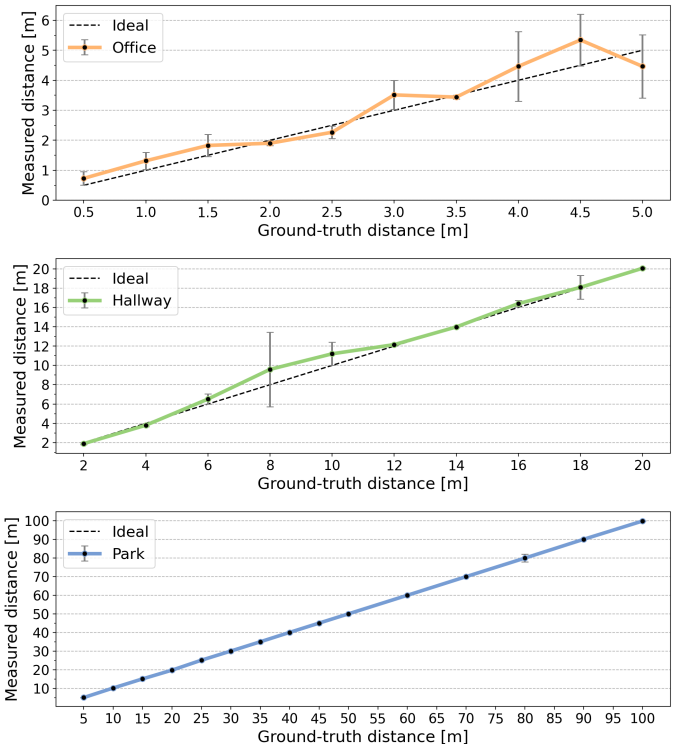

Fig. 7. iCDE* distance estimation results displaying median value and mean absolute error.

(179.9 uWs). Compared with the previously proposed phase-based ranging solutions in [21], [22], our implementation consumes less energy, as it is sampling phase angles on only 15 different frequencies instead of 200.

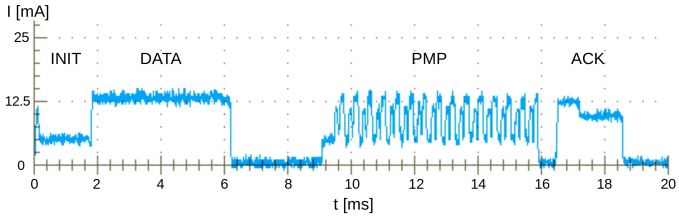

Fig. 8. Radio's power consumption during transmission routine measured with the onboard shunt resistor. INIT: initialization, DATA: transmission of a data packet, PMP: PM process, ACK: acknowledgment.

VI. CONCLUSION

In this article, we introduced two new methods of phase-based distance estimation that are compatible with the IEEE 802.15.4 TSCH protocol. By seamlessly adding a phase measurement process in the timeslot, the proposed method is able to estimate the distance between two devices after each data packet is sent. The acquisition rate of the distance estimations can be high, and we suggest using 5 consecutive measurements to filter out possible outliers. Although the timeslot is extended by 10 ms and the energy consumption increases, in return, we can estimate a distance with a median error of 0.26 m and an accuracy of 0.31 m for indoor scenarios and a median error of 0.05 m and an accuracy of 0.05 m

for outdoor scenarios. The proposed improvement of iCDE algorithm, where only 15 samples are obtained instead of 200, further improves the time efficiency and reduces the energy consumption of the distance estimation technique. The implementation of the proposed methods on low-cost off-the-shelf devices offers a cost-effective solution for IoT networks, where localization functionality is required alongside responsive and reliable communication capabilities of the TSCH network.

REFERENCES

[1] C. De Lima, D. Belot, R. Berkvens, A. Bourdoux, D. Dardari, M. Guillaud, M. Isomursu, E.-S. Lohan, Y. Miao, A. N. Barreto, M. R. K. Aziz, J. Saloranta, T. Sanguanpuak, H. Sarieddeen, G. Seco-Granados, J. Suutala, T. Svensson, M. Valkama, B. Van Liempd, and H. Wymeersch, "Convergent Communication, Sensing and Localization in 6G Systems: An Overview of Technologies, Opportunities and Challenges," *IEEE Access*, vol. 9, pp. 26 902–26 925, 2021.

[2] J. Wang, N. Varshney, C. Gentile, S. Blandino, J. Chuang, and N. Golmie, "Integrated Sensing and Communication: Enabling Techniques, Applications, Tools and Data Sets, Standardization, and Future Directions," *IEEE Internet of Things Journal*, vol. 9, no. 23, pp. 23 416–23 440, 2022.

[3] J. A. Zhang, M. L. Rahman, K. Wu, X. Huang, Y. J. Guo, S. Chen, and J. Yuan, "Enabling Joint Communication and Radar Sensing in Mobile Networks—A Survey," *IEEE Communications Surveys Tutorials*, vol. 24, no. 1, pp. 306–345, 2022.

[4] R. Marini, K. Mikhaylov, G. Pasolini, and C. Buratti, "Low-Power Wide-Area Networks: Comparison of LoRaWAN and NB-IoT Performance," *IEEE Internet of Things Journal*, vol. 9, no. 21, pp. 21 051–21 063, 2022.

[5] S. J. Danbatta and A. Varol, "Comparison of Zigbee, Z-Wave, Wi-Fi, and Bluetooth Wireless Technologies Used in Home Automation," in *2019 7th International Symposium on Digital Forensics and Security (ISDFS)*, 2019, pp. 1–5.

[6] "IEEE Standard for Low-Rate Wireless Networks," *IEEE Std 802.15.4-2015 (Revision of IEEE Std 802.15.4-2011)*, pp. 1–709, 2016.

[7] Milica Lekic, Gordana Gardasevic, and Milan Mladen, "Experimental evaluation of multi-PHY 6TiSCH networks," *ITU Journal on Future and Evolving Technologies*, vol. 3, no. 2, pp. 470–482, 2022. [Online]. Available: https://www.itu.int/pub/S-JNL-VOL3.ISSUE2-2022-A36

[8] S. Sadowski, P. Spachos, and K. N. Plataniotis, "Memoryless Techniques and Wireless Technologies for Indoor Localization With the Internet of Things," *IEEE Internet of Things Journal*, vol. 7, no. 11, pp. 10 996–11 005, 2020.

[9] V. Bianchi, P. Ciampolini, and I. De Munari, "RSSI-Based Indoor Localization and Identification for ZigBee Wireless Sensor Networks in Smart Homes," *IEEE Transactions on Instrumentation and Measurement*, vol. 68, no. 2, pp. 566–575, 2019.

[10] M. T. Hoang, B. Yuen, X. Dong, T. Lu, R. Westendorp, and K. Reddy, "Recurrent Neural Networks for Accurate RSSI Indoor Localization," *IEEE Internet of Things Journal*, vol. 6, no. 6, pp. 10 639–10 651, 2019.

[11] S. Sadowski and P. Spachos, "RSSI-Based Indoor Localization With the Internet of Things," *IEEE Access*, vol. 6, pp. 30 149–30 161, 2018.

[12] S. Lanzisera, D. Zats, and K. S. J. Pister, "Radio Frequency Time-of-Flight Distance Measurement for Low-Cost Wireless Sensor Localization," *IEEE Sensors Journal*, vol. 11, no. 3, pp. 837–845, 2011-03.

[13] S. Lanzisera, D. T. Lin, and K. S. J. Pister, "RF Time of Flight Ranging for Wireless Sensor Network Localization," in *2006 International Workshop on Intelligent Solutions in Embedded Systems*, 2006, pp. 1–12.

[14] M. D. Bedford and G. A. Kennedy, "Evaluation of ZigBee (IEEE 802.15.4) Time-of-Flight-Based Distance Measurement for Application in Emergency Underground Navigation," *IEEE Transactions on Antennas and Propagation*, vol. 60, no. 5, pp. 2502–2510, 2012.

[15] L. Flueratoru, S. Wehrli, M. Magno, E. S. Lohan, and D. Niculescu, "High-Accuracy Ranging and Localization With Ultrawideband Communications for Energy-Constrained Devices," *IEEE Internet of Things Journal*, vol. 9, no. 10, pp. 7463–7480, 2022.

[16] W. Kluge and E. Sachse, "System, method, and circuit for distance measurement between two nodes of a radio network," patentus 8 644 768B2, 2014.

[17] P. Zand, J. Romme, J. Govers, F. Pasveer, and G. Dolmans, "A high-accuracy phase-based ranging solution with Bluetooth Low Energy (BLE)," in *2019 IEEE Wireless Communications and Networking Conference (WCNC)*, 2019, pp. 1–8.

[18] M. Technology. AT86RF233 - Complete Datasheet. [Online]. Available: https://ww1.microchip.com/downloads/en/DeviceDoc/Atmel-8351-MCU_Wireless-AT86RF233_Datasheet.pdf

[19] M. Pelka, C. Bollmeyer, and H. Hellbrück, "Accurate radio distance estimation by phase measurements with multiple frequencies," in *2014 International Conference on Indoor Positioning and Indoor Navigation (IPIN)*, 2014-10, pp. 142–151.

[20] O. Oshiga, A. Ghods, S. Severi, and G. Abreu, "Efficient Slope Sampling Ranging and Trilateration Techniques for Wireless Localization," p. 6, 2015.

[21] G. von Zengen, Y. Schröder, S. Rottmann, F. Büsching, and L. C. Wolf, "No-cost distance estimation using standard WSN radios," in *IEEE INFOCOM 2016 - The 35th Annual IEEE International Conference on Computer Communications*, 2016, pp. 1–9.

[22] Y. Schröder, D. Reimers, and L. Wolf, "Accurate and Precise Distance Estimation from Phase-Based Ranging Data," in *2018 International Conference on Indoor Positioning and Indoor Navigation (IPIN)*, 2018, pp. 1–8.

[23] P. Zand, A. Duzen, J. Romme, J. Govers, C. Bachmann, and K. Philips, "A high-accuracy concurrent phase-based ranging for large-scale dense BLE network," in *2019 IEEE 30th Annual International Symposium on Personal, Indoor and Mobile Radio Communications (PIMRC)*, 2019, pp. 1–7.

[24] O. Oshiga, S. Severi, and G. T. F. de Abreu, "Superresolution Multipoint Ranging With Optimized Sampling via Orthogonally Designed Golomb Rulers," *IEEE Transactions on Wireless Communications*, vol. 15, no. 1, pp. 267–282, 2016.

[25] R. Ayyalasomayajula, D. Vasisht, and D. Bharadia, "BLoc: CSI-based accurate localization for BLE tags," in *Proceedings of the 14th International Conference on Emerging Networking EXperiments and Technologies*. ACM, 2018, pp. 126–138.

[26] S. Duquennoy, A. Elsts, B. A. Nahas, and G. Oikonomo, "TSCH and 6TiSCH for Contiki: Challenges, Design and Evaluation," in *2017 13th International Conference on Distributed Computing in Sensor Systems (DCOSS)*, 2017, pp. 11–18.

[27] T. Chang, T. Watteyne, K. Pister, and Q. Wang, "Adaptive synchronization in multi-hop TSCH networks," *Computer Networks*, vol. 76, pp. 165–176, 2015. [Online]. Available: https://linkinghub.elsevier.com/retrieve/pii/S1389128614003922

[28] Contiki-NG, the os for next generation iot devices. [Online]. Available: https://www.contiki-ng.org/

[29] LOG-a-TEC by SensorLab. [Online]. Available: https://log-a-tec.eu/

[30] Y. Schröder and L. Wolf, "InPhase: Phase-based Ranging and Localization," *ACM Transactions on Sensor Networks*, vol. 18, no. 2, pp. 1–39, 2022.

Grega Morano (Student Member, IEEE) received his M.Sc. degree in electrical engineering from the University Of Ljubljana, in 2021. He currently works as a research assistant at the Department of Communication Systems at Jožef Stefan Institute, Ljubljana, and is pursuing his Ph.D. in Information and Communication Technologies at the Jožef Stefan International Postgraduate School. Among his research interests are IoT communication protocols, integrated sensing and communication, wireless sensor networks and wireless experimental testbeds.

Ke Guan (Senior Member, IEEE) received B.E. degree and Ph.D. degree from Beijing Jiaotong University in 2006 and 2014, respectively. He is a Professor in the State Key Laboratory of Rail Traffic Control and Safety & School of Electronic and Information Engineering, Beijing Jiaotong University. In 2015, he has been awarded a Humboldt Research Fellowship for Postdoctoral Researchers. In 2009, he was a Visiting Scholar with Universidad Politécnica de Madrid, Spain. From 2011 to 2013, he was a Research Scholar with the Institut für Nachrichtentechnik (IfN) at Technische Universität Braunschweig, Germany. From September 2013 to January 2014, he was invited to conduct joint research at Universidad Politécnica de Madrid, Spain. He has authored/coauthored two books and one book chapter, more than 200 journal and conference papers, and four patents. His current research interests include measurements and modeling of wireless propagation channels, high-speed railway communications, vehicle-to-x channel characterization, and indoor channel characterization for high-speed short-range systems including future terahertz communication systems.

Dr. Guan is the pole leader of EURNEX (European Railway Research Network of Excellence). He was the recipient of a 2014 International Union of Radio Science (URSI) Young Scientist Award. His papers received ten Best Paper Awards, including IEEE vehicular technology society Neal Shepherd memorial best propagation paper award in 2019 and 2022. He is an Editor of IEEE Vehicular Technology Magazine, IEEE ACCESS, IET Microwave, Antenna and Propagation, Physical Communication, and a Guest Editor of the IEEE Transactions on Vehicular Technology and IEEE Communication Magazine. He serves as a Publicity Chair in PIMRC 2016, the Publicity Co-Chair in ITST 2018, the Track Co-Chair in EuCNC, the International Liaison of EUSIPCO 2019, the Session Convener of EuCAP 2015-2022, and a TPC Member for many IEEE conferences, such as Globecom, ICC, and VTC. He has been a delegate in 3GPP and a member of the IC1004 and CA15104 initiatives.

Andrej Hrovat (Member, IEEE) received his B.Sc. and M.Sc. degrees in electrical engineering from the University of Ljubljana in 2004 and 2008 and finished his Ph.D. at the Jozef Stefan International Postgraduate School in 2011. He is with the Department of Communication Systems at the Jožef Stefan Institute since 2004, at present holding the position of a senior research fellow.

His research and working experience are in the field of telecommunications, focusing on development and performance analysis for fixed and mobile systems, including terrestrial, stratospheric, and satellite systems, and radio-channel modeling for fixed and mobile narrowband and broadband radio communication systems. He works on several projects connected with professional mobile communication systems, 2/3/4G, WiFi and WiMAX technologies, satellite and sensor networks, including several COST actions, Framework Program projects, H2020 projects, European Space Agency (ESA) projects, and numerous national research and application projects.

Dr. Hrovat is the author or co-author of more than 80 peer-reviewed journal and conference papers, serves as a journal editorial board member and guest editor, reviewer for several international impact-factor journals, and is a TCP member for various international conferences and workshops.

Tomaž Javornik (Member, IEEE) received his B.Sc., M.Sc., and Ph.D. degrees in electrical engineering from the University of Ljubljana, Ljubljana, Slovenia, in 1987, 1990, and 1993, respectively. He is a Scientific Counsellor with the Communication Systems Department, Jozef Stefan Institute, Ljubljana, Slovenia, and an Assistant Professor with the Jozef Stefan International Postgraduate School, Ljubljana. He participated in several COST and Framework Programme projects. He has coauthored more than 100 refereed journal and conference papers and several books and book chapters in the field of mobile and wireless communications. He holds two international patents.

His research experience is in the field of telecommunications, focusing on the development and performance analysis of fixed and mobile systems, radio-channel measurements, modeling and simulations and in indoor localization.

Dr. Javornik serves as a TPC Member or a reviewer for several IEEE conferences and journals.